Effect of Pressure on Pedal Motion in Stilbene Molecular Crystals and Its Dependence on the Crystallographic Site

N. Arul Murugan[†] and S. Yashonath*[,‡]

Solid State and Structural Chemistry Unit, Indian Institute of Science, Bangalore, India - 560 012, and Condensed Matter Theory Unit, Jawaharlal Nehru Centre for Advanced Scientific Research, Bangalore, India - 560 064

Received: November 22, 2004; In Final Form: April 21, 2005

We report computer simulation of a stilbene molecular crystal as a function of pressure up to 4 GPa. Molecular structure and the crystal structure of stilbene have been characterized by calculating the radial distribution function and dihedral angle distribution, features associated with pedal motion and cell parameters. Results suggest that the population of minor conformer at site 2 disappears altogether above 1.25 GPa. In contrast, the population of minor conformer at site 1 remains at around 12%. Pedal motion is not observed beyond a pressure of 0.8 and 1.4 GPa at site 1 and site 2, respectively. Specific heat and compressibility exhibit an anomaly around 1.25 GPa. The anomaly seems to be associated with the disappearance of pedal motion at site 2. Initially, increase in pressure leads to an increase in the magnitude of lattice energy, but beyond 0.5 GPa it decreases.

1. Introduction

Ideally, crystals are perfectly ordered solids. However, at room temperature considerable degree of disorder exists. This could be of two kinds: static and dynamic. At any finite temperature, thermal motion leads to some degree of dynamic disorder. Normally the amplitude of motion due to thermal energy is significantly smaller than the intermolecular separation. However, in some solids the thermal motion can be large compared to the distance of intermolecular separation. This is the case, for example in inorganic superionic conductors such as AgI, $Na_{1+x}Zr_2Si_xP_{3-x}O_{12}$ (Nasicons) with $0 \leq x \leq 3$ or molecular crystals such as biphenyl or stilbene.

Study of disorder in crystalline solids has attracted much attention in recent times.[1] The principal motivation arises from the fact that the existence of disorder alters mechanical, thermodynamic, optical, electronic, and spectroscopic properties.[2−4]

Stilbene provides an interesting example of disorder due to torsional motion.[5,6] Crystallographic studies with X-rays and neutron have shown that the crankshaft motion (often referred to as pedallike motion) occurs at room temperature in crystalline stilbene.[6] Crystal structure analysis of stilbene at room temperature and 1 atm pressure suggests that C═C ethylene bond length interconnecting two phenyl rings is shorter than the C═C bond length in the ethylene (C_2H_4) molecule.[7] A more careful analysis by Ogawa and co-workers[7] of stilbene and its derivatives suggests that the shortening of the ethylene double bond is an artifact having its origin in the pedallike motion of stilbene molecules. Such pedallike motion can arise from torsional rotation through an angle ϕ around the C−Ph bond. Proof of pedallike motion has been obtained from X-ray diffraction studies.[6] Onset of such motion occurs first at the crystallographic site 2 where a significant fraction of molecules are seen to be in the $\phi = \pm 180°$ conformations referred to as the minor conformer (see Figure 1) as compared to major conformer ($\phi = 0°$). In the gas phase, minor and major conformers are identical and there is no difference in energy between them. In the crystals, the intermolecular interactions arising from crystal packing lead to a less efficient packing of the minor conformer. This is responsible for the observed energy difference. The minor conformer will have a higher energy than the major conformer ($\phi = 0°$). Previously, molecular mechanics calculation by Galli et al.[8] suggests that the barrier to torsional rotation at site 2 is higher than at site 1. However, recent variable shape Monte Carlo simulations[9] suggest that the barrier obtained from molecular mechanics calculations[8] are unrealistically large. It appears that the local expansion of the lattice and reorientation of the neighbors of a molecule performing pedallike motion can be important and is responsible for lowering of activation energies associated with pedallike motion. These Monte Carlo calculations[9] suggest that the activation energy for pedallike motion at site 2 is 10.38 kJ/mol, significantly smaller than 63.4 kJ/mol suggested by molecular mechanics calculations. Luminescence studies by Ghosal et al.[10] and Raman phonon spectroscopic studies by Charabarthi and Mishra[11] suggest the possible existence of two transitions one near 110 K and another near 220 K. Monte Carlo simulations[9] suggest that these two transitions may be associated with the onset of pedallike motion at site 2 which occurs close to 170 K and at site 1 which occurs at relatively higher temperatures.

Although there exist a large number of studies investigating the nature of disorder as a function of temperature, there are few studies investigating the effect of pressure on stilbene crystals. Takeshita et al.[12] have recently reported Raman measurements on stilbene crystals as a function of pressure. They have looked at changes in Raman bands from 0.1 to 6 GPa in steps of 0.2 GPa. On the basis of the variation of the frequency and the half-width of the Raman bands due to inter- and intramolecular vibrations within stilbene crystals, they

* To whom correspondence should be addressed. E-mail: yashonat@sscu.iisc.ernet.in.
[†] Jawaharlal Nehru Centre for Advanced Scientific Research.
[‡] Indian Institute of Science.

10.1021/jp044676i CCC: $30.25
Published on Web 05/25/2005

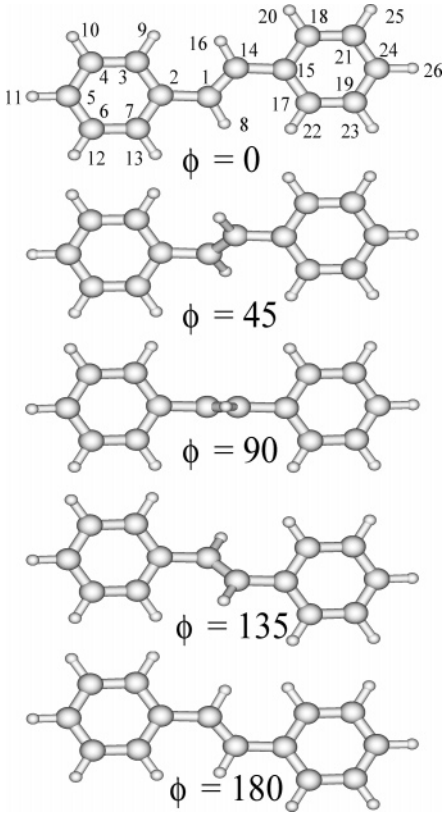

Figure 1. Pedallike motion in stilbene.

conclude that there are two second-order phase transitions at 1.5−2 and 4 GPa. The origin of these is, however, not clear.

Molecular simulations have been employed in the study of the crystal structure of molecular solids as well as for understanding solid−solid structural transitions since the pioneering work of Parrinello and Rahman[13] who proposed the use of a variable shape simulation cell instead of the usual cubic periodic boundary condition. Since then, this method has been successfully used to study structural phase transformations in a number of systems such as CF_4,[14] CH_4,[15] N_2,[16] acetylene,[17] ice,[18] etc. These studies have demonstrated that computer simulation methods[19,20] such as molecular dynamics and Monte Carlo provide an alternative technique for the simulation of crystal structure and structural phase transformations. They provide valuable additional information such as atomic or microscopic properties that cannot be directly obtained from experiments. It is also possible to study the effect of extreme pressures and temperatures. Frequently, these methods have been used to study the effect of change in just one parameter, e.g., mass, without corresponding changes in other parameters such as, for example, in size. Such studies are not easily carried out experimentally. These techniques do have some limitations. Finite size effects are known due to the small size of the system employed in the simulations.[18,21,22] The small size of the system employed in the simulations lead to differences in the transition pressures or temperatures. For example, Velardez, Alavi, and Thompson[21] found that the melting temperature of ammonium dinitramide undergoes the transition at around 474−490 K instead of the experimentally observed value of 475 K. Simulations of solid poly(tetrafluoroethylene) by Sprik, Rothlisberger, and Klein[22] found that the order−disorder transition takes place at around 725 K instead of the experimentally observed value of 575 K. Hysteresis during changes from one phase to another in simulated systems has also been reported.[14,21−23] Despite these limitations which are of minor nature, computer simulation has proved to be a useful tool in the study of solids.

TABLE 1: ΔH for Site 1 and Site 2

site	ΔH, kJ/mol
site 1	18.8
site 2	11.6

Here, we report a detailed simulations of stilbene crystals at room temperature as a function of pressure. Simulations have been carried out in isothermal−isobaric ensemble with variable shape simulation cell. We report properties that provide an insight into the nature of disorder and its dependence on pressure.

2. Methods

2.1. Intermolecular Potential. The atom−atom potential of Williams[24] with suitable modification[9] has been used to model intermolecular interactions in stilbene. We recently employed this potential to carry out a temperature dependent study of stilbene.[9] The potential parameters have been derived based on data related to experimental crystal structures of 134 hydrocarbon molecules having 5−16 carbon atoms and eight heats of sublimation. The potential is of 6-exp type with $N_a = 26$ interaction sites per stilbene molecule (see eq 1).

$$\phi(r_{ij,\mu\nu}) = -\frac{A_{\mu\nu}}{(r_{ij,\mu\nu})^6} + B_{\mu\nu}\exp(-C_{\mu\nu}r_{ij,\mu\nu}) \qquad (1)$$

Here i,j refer to molecular indices and μ,ν to atomic indices. The well depth of the potential has been reduced by multiplication with 0.8 so as to obtain a better agreement of the simulated results with experiment. Previous calculations using the Williams potential suggest that the intermolecular interaction has a greater well depth and leads to slower dynamics as compared to experiments.[25] The present reduction in well depth is therefore expected to lead to better agreement with experiment. Figure 1 shows the numbering employed for the stilbene molecule.

2.2. Intramolecular Potential. We are not aware of any suitable intramolecular potential function derived experimentally or theoretically to model the pedallike motion of the stilbene molecule. We have, therefore, derived an intramolecular potential function as described in a recent paper on stilbene[9] based on ab initio calculations carried out at Hartree−Fock level with 6−31 g(d) basis set as implemented in Gaussian98.[26] This calculation involves a set of constrained optimization, where the dihedral angles ϕ_1 for rotation around C(1)−C(2) and ϕ_2 for rotation around C(14)−C(15) bond are constrained in such a way that $\phi_1 = \phi_2$. Here the direction of rotations are such that the two phenyl rings are parallel to each other after both rotations. The ab initio energies were calculated as a function of the dihedral angle in steps of 10°.

However, ab initio energies generally overestimate the values of the energy barriers, and therefore the energies were scaled by a factor of 0.1. A function of the form (see eq 2) was fitted to these ab initio energies.

$$V_{\text{intra}}(\phi) = c_0 + c_1(1.0 - \cos(2\phi)) + c_2(1.0 - \cos(4\phi)) + c_3(1.0 - \cos(6\phi)) \qquad (2)$$

where ϕ is specified in radians. The constants c_0, c_1, c_2, and c_3 were determined by the fit. These are listed in Table 2. Note that the torsional rotation is applied on one of the phenyl rings and the other torsional rotation on the other phenyl ring. This

TABLE 2: Intermolecular and Intramolecular Potential Parameters Used in the Simulation of Stilbene

Intermolecular Potential			
type	A, kJ/mol Å^6	B, kJ/mol	C, Å^{-1}
C−C	1314.17	190861.6	3.60
C−H	538.68	44696.64	3.58
H−H	220.81	10467.2	3.56

Intramolecular Potential			
c_0, kJ/mol	c_1, kJ/mol	c_2, kJ/mol	c_3, kJ/mol
0.04168	1.19446	−0.36037	−0.01116

coupled with overall rotation of the molecule as a whole leads to facile pedallike motion in stilbene.

Intramolecular energy has two principal contributions: (i) conjugation energy which stabilizes the planar conformation due to π-overlap and (ii) repulsion between ethylenic hydrogens and the ortho-hydrogens which destabilizes the planar conformation. (iii) In the solid phase, the role of intermolecular energy in the resulting conformation of the stilbene is also important. The resulting conformation is due to these three competing interactions.

2.3. Variable Shape NPT-MC Simulations. Simulations have been carried out in isothermal−isobaric or NPT ensemble with variable shape simulation[13] cell using the Monte Carlo method and the importance sampling algorithm of Metropolis.[27] The simulation cell is represented by 6 degrees of freedom. Seven degrees are associated with the each molecule: three with translation, three with rotation, and one with the torsional motion involving the two dihedral angles, ϕ_1 and ϕ_2 (since $\phi_1 = \phi_2$). For more details, see refs 9 and 28.

Here the total interaction energy of the stilbene crystal has two components.

$$U = U_{\text{intra}} + U_{\text{inter}} = \sum_{i=1}^{N} V_{\text{intra}}(\phi_i) + \frac{1}{2}\sum_{i=1}^{N}\sum_{j=1}^{N}\sum_{\mu=1}^{N_a}\sum_{\nu=1}^{N_a}\phi(r_{ij,\mu\nu}) \quad (3)$$

where U_{intra} is the total intramolecular energy and U_{inter} is the total intermolecular energy.

3. Computational Details

Simulations have been carried out on 3 × 7 × 3 unit cells with 252 stilbene molecules. The initial configuration and the lattice parameters for the simulation at 150 K have been taken from the X-ray structure at 113 K reported by Hoekstra et al.[29] (space group = $P2_1/a$, $Z = 4$). The temperature has been increased gradually to 300 K. Then the pressure has been increased gradually from 1 atm to 4.0 GPa.

Each Monte Carlo move (MCM) consists of a random displacement, a rotation around a randomly selected axis by a random amount and a torsional rotation again chosen randomly around the C−Ph bonds. One Monte Carlo step (MCS) consists of an attempted MCM once on each of the N molecules and attempted displacement of each of the three simulation cell vectors **a**, **b**, and **c**. Displacements have been adjusted to obtain an acceptance ratio of 0.40 to ensure that the sampling over the configurational phase space is efficient. Calculations were carried out at the pressures 1 atm, 0.2, 0.4, 0.6, 0.8, 1.0, 1.25, 1.4, 2.0, 3.0, and at 4.0 GPa. Simulations at a given pressure and temperature is carried out for 26000 MCS which include 6000 MCS for equilibration. A center of mass(com)-com cutoff of 13 Å has been employed.

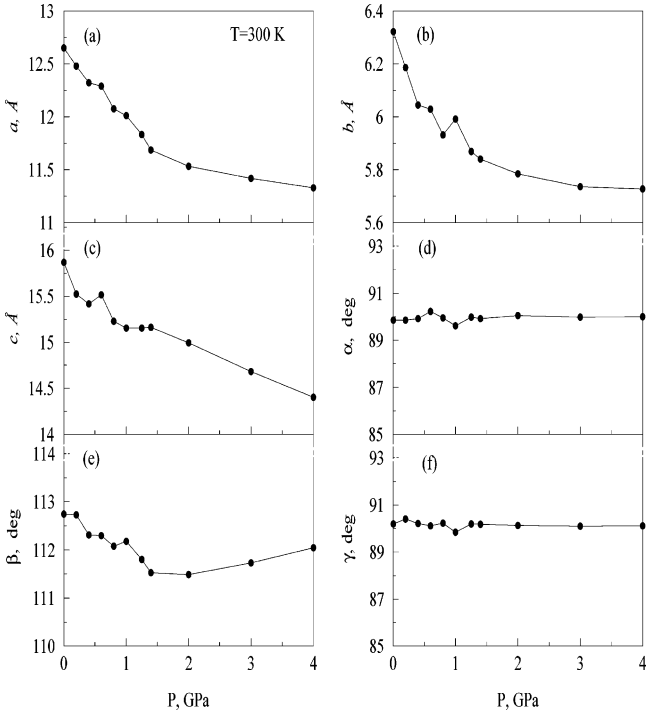

Figure 2. Variation of cell parameters as function of pressure up to 4.0 GPa at 300 K: (a) *a*, (*b*) *b*, (*c*) *c*, (*d*) α, (*e*) β, (*f*) γ.

4. Results and Discussion

In Figure 2 the variation of lattice parameters *a*, *b*, *c*, α, β, and γ with pressure at 300 K is shown. With the increase in hydrostatic pressure as expected all the three parameters *a*, *b*, and *c* contract. Note that the largest variation in *a*, *b*, and *c* is seen below 1.5 GPa. Beyond this pressure only small changes in lattice parameters are seen. This is also true of β. The changes in *a*, *b*, and *c* on increase in pressure from 1 atm to 4.0 GPa are 12.0, 10.0, and 8.7%, respectively. Increase in pressure also causes significant change in unit cell volume especially between 1 atm and 1.5 GPa (see Figure 3). The reduction in volume is large, 25%. The derivative of V/V_0 with pressure where V_0 is the volume at 1 atm is also shown in Figure 3. This has been obtained by numerical differentiation of V/V_0 vs pressure using forward difference method. The derivative has large (negative) value initially but approaches zero and by 1.5 GPa most of the changes has already taken place. A lowering of the derivative is seen near 1.25 GPa. Reasons for this will become clear when the changes in molecular conformation is discussed.

Variation of U_{total} with pressure is shown in Figure 4 for site 1, site 2 as well as the combined average. U_{inter} has a predominant contribution to U_{total} and U_{intra} has only a marginal contribution. With increase in pressure magnitude of U_{total} increases initially but later decreases. This increase is about 5.0 kJ/mol. The minimum occurs at 0.5 GPa. Increase in pressure beyond 0.5 GPa leads to decrease in magnitude of U_{total} and U_{inter}. A similar minimum has been observed in the case of biphenyl,[30] adamantane,[31] and *p*-terphenyl[32] when pressure is applied. It is possible that this is an universal behavior. This behavior may be understood in the following way. In most room temperature molecular crystals a certain amount of excess free volume is present. The availability of this excess volume is due to relatively weak intermolecular interactions largely due to van der Waals interactions. On application of pressure, there is an overall decrease in the intermolecular distances which leads to a more favorable intermolecular interactions and packing efficiency, thus causing an increase in magnitude of U_{inter}.

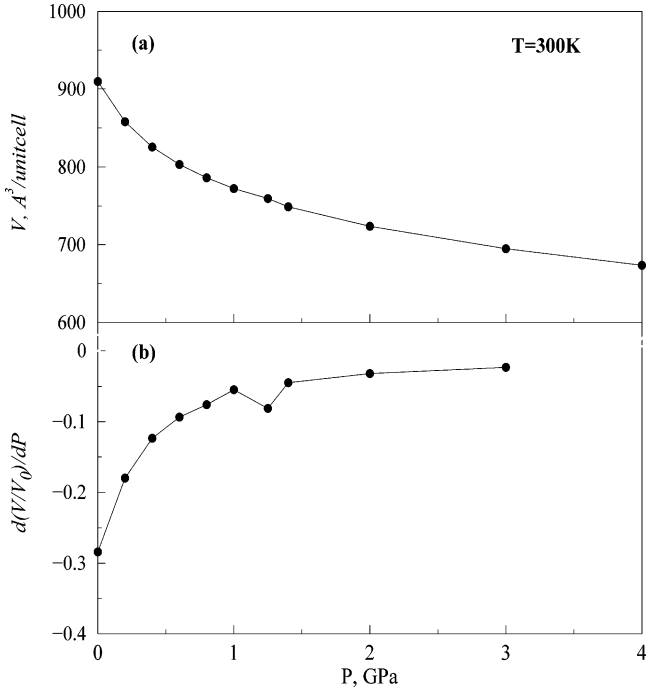

Figure 3. (a) Variation of unit cell volume. (b) $d(V/V_{1atm})/dP$ as a function of pressure.

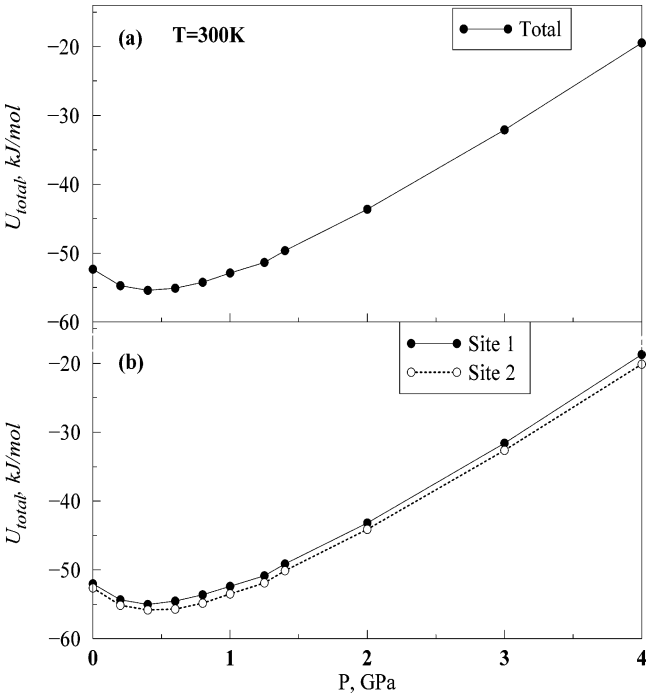

Figure 4. Variation of U_{total} (a) for all molecules (b) and site 1 and site 2 molecules as a function of pressure.

Usually, the contribution from U_{intra} is relatively small and this trend in U_{inter} is also seen in U_{total}. Further, increase in pressure beyond this value leads to unfavorable interactions between neighboring molecules. This causes an increase in U_{total} or a decrease in the magnitude of U_{total}.

In Figure 4b we show the variation of U_{total} with pressure for site 1 and site 2. We see that the difference in energy between site 1 and site 2 molecules neither increases nor decreases but remains constant with molecules at site 1 always having a higher energy. Previously, it has been shown that the interaction energy with the lattice of site 1 molecules and site 2 molecules differ by about 1.0 kJ/mol. Further, at low temperatures, this difference

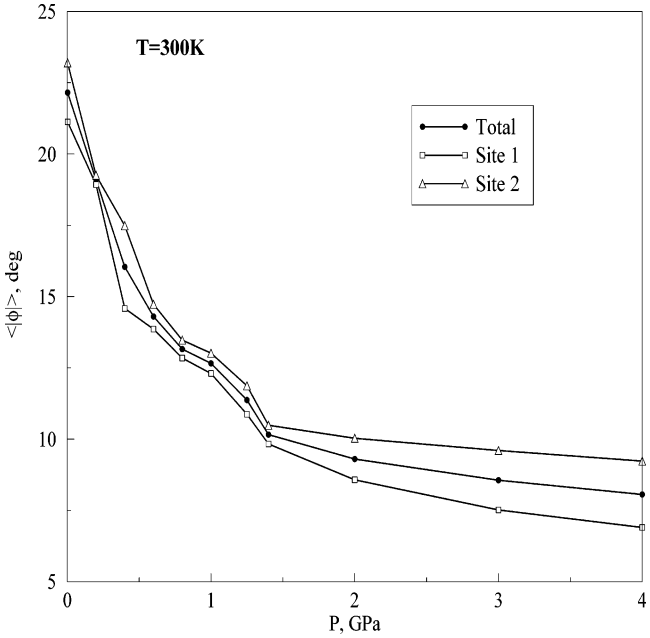

Figure 5. Variation of $\langle|\phi|\rangle$ as a function of pressure for site 1, site 2, and for both crystallographic sites.

increases. This may be compared with molecular crystals such as adamantane. In the latter, this difference in energy is nearly zero at 1 atm pressure but increases to significant degree at high pressures.

It is known that stilbene undergoes torsional motion leading to crankshaft or pedal motion. We have examined here the variation of the dihedral angle with pressure (see Figure 5). We have also shown this variation for site 1 and site 2 separately. Note that this variation is largest between 1 atm and 1.5 GPa. Beyond this pressure little variation in $\langle|\phi|\rangle$ is seen. This is consistent with large magnitude of $d(V/V_0)/dP$ up to 1.5 GPa. It suggests that the large change in volume with pressure below 1.5 GPa arises from increasing planarity of the stilbene molecules with pressure. Previous studies by a number of groups[33,34] has shown that a small fraction of stilbene molecules exist in another conformation which is obtained by a 180° torsional rotation of the usual conformer. This $\phi \approx 180°$ conformer is referred to as the minor conformer, and predominant conformation for which ϕ is ≈ 0 ° is referred to as major conformer. During pedallike motion, a stilbene molecule assumes conformations with values of ϕ that are between 0° and 180°; the conformation with $\phi = 90°$ may be expected to correspond to the transition state for which the potential energy is maximum. The reduction in the value of $|\phi|$ in Figure 5 suggests that there are fewer torsional rotations leading to pedallike motion and also that there is a reduction in the amplitude of the torsional motion. Radial distribution functions (rdfs) for com-com, C−C, C−H, and H−H are shown in Figure 6 at different pressures. At 1 atm, the rdf does not exhibit sharp well-defined peaks in any of the rdfs. Even the com-com rdf shows considerable fluidlike character, suggesting thereby that pedallike motion at 300 K is accompanied by significant amount of displacement of the molecular center of mass. On increase in pressure the rdfs develop well-defined features suggestive of an increase in order or decrease in disorder. This behavior along with changes in $\langle\phi\rangle$ suggests that disorder arising out of torsional motion has significantly reduced by 1.5 GPa. The distribution of dihedral angle at various pressures are shown in Figure 7. At low pressures the distribution shows the existence of major conformers ($\phi = 0°$) and minor conformers ($\phi =$

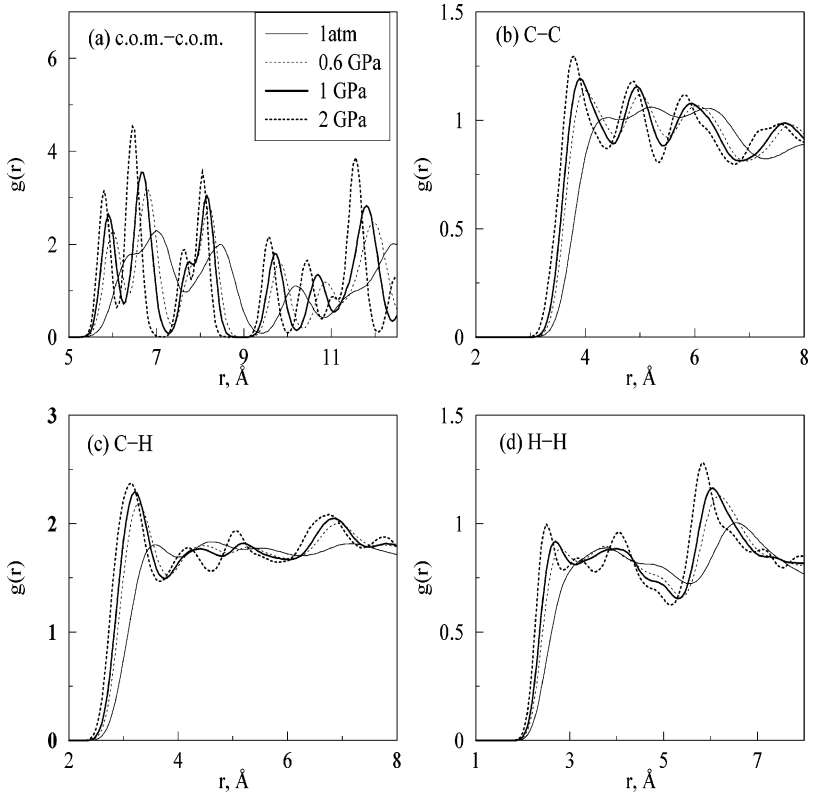

Figure 6. Variation of various radial distribution functions as a function of pressure: (a) com-com, (b) C−C, (c) C−H, (d) H−H.

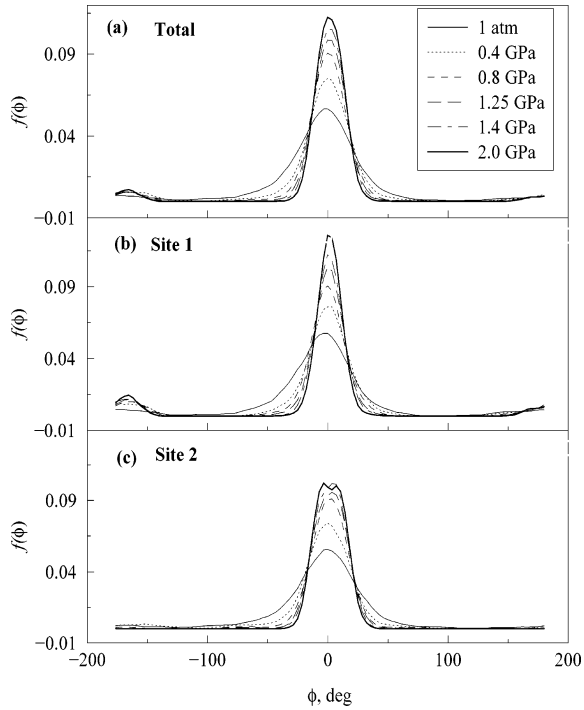

Figure 7. $f(\phi)$ as a function of pressure at 300 K averaged over (a) both the crystallographic sites, (b) site 1, (c) site 2.

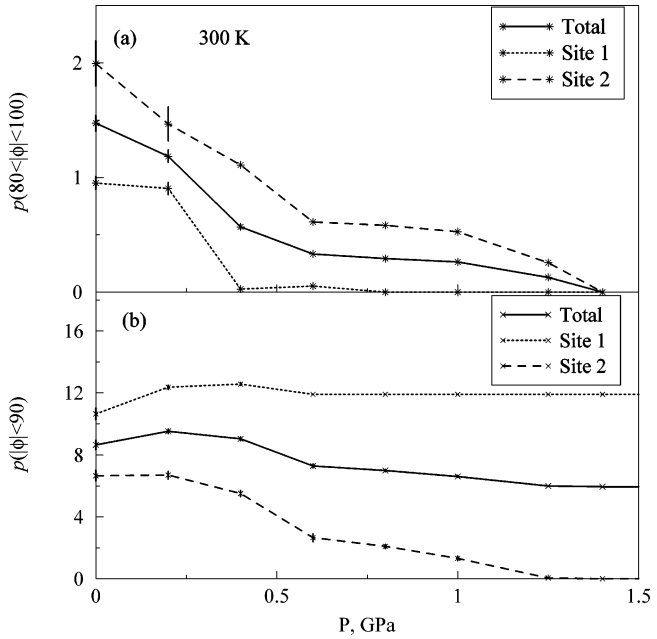

Figure 8. (a) Percentage population of molecules in the transition state. The error in calculation at $P = 0.2$ GPa is shown. Error is lower at higher pressures. (b) Percentage population of minor conformers as a function of pressure at 300 K averaged over site 1 and site 2 molecules and over both the crystallographic sites. Error in computed quantity is shown.

±180°). In addition to these, there is a small but nonnegligible population of stilbene molecules which can be classified neither under major nor under minor conformers. These molecules have a dihedral angle neither close to 0° nor to ±180°. The nonzero population of molecules at $\phi = \pm 90°$ provides an estimate of the fraction of stilbene molecules in the process of transition from major to minor or to minor to major conformation. Note that by 1.5 GPa, $f(\phi)$ has zero population at ±90°, suggesting thereby that by this pressure pedallike motion ceases. Figure 7b and 7c show the distributions of dihedral angle for site 1 and site 2, respectively.

To obtain a more accurate estimate of the pressure at which the pedallike motion ceases to exist, we plot fraction of molecules with dihedral angle $80° < |\phi| < 100°$ as a function of pressure. These are shown in Figure 8a for site 1 and site 2 separately as well as the combined average. Note that at site 1 the pedallike motion nearly ceases to exist by 0.4 GPa. In any

case, by 0.8 GPa there is no trace of pedallike motion at site 1. In the case of site 2, pedallike motion is not seen at pressures higher than 1.4 GPa. Thus, it is evident that the pedallike motion ceases to exist at site 1 at a pressure that is lower than for site 2. Previously, X-ray diffraction studies of Ogawa and coworkers[6] as well as Monte Carlo simulation of ours[9] have shown that the onset of pedallike motion at site 1 at atmospheric pressure occurs at a higher temperature as compared to the stilbene at site 2. From the simulation studies, we find that the activation energy for site 1 is higher than site 2. The result obtained here that pedal motion ceases at site 1 at a lower pressure as compared to site 2 is consistent with the difference in the temperature at which the onset of pedal motion takes place and the difference in activation energy.

So far, we have looked at the dependence of the rate of conversion between minor and major conformers on pressure. We now look at the variation or dependence of population of minor conformers on pressure at site 1, site 2, and the overall average. The population of major (minor) conformers is defined as those stilbene molecules satisfying $|\phi| < 90°$ ($|\phi| > 90°$) and have been obtained by integration of $f(\phi)$ shown in Figure 7. Figure 8b shows a plot of percentage population of minor conformers, $p(|\phi| < 90°)$ as a function of pressure. Initially, there is a small increase in the population of minor conformers at site 1. Site 2 shows no such increase. Beyond 0.2 GPa, there is a decrease in the population of minor conformers in site 2. As we have already noted, by 1.4 GPa interconversion between two conformers is reduced to zero. Figure 8b shows that by about 1.25 GPa almost all minor conformers have converted to major conformers at site 2. Thus, the minor conformers population at site 2 is reduced to zero at about the pressure by which the interconversion stops. In the case of site 1, the situation is quite different. As we have seen, (see Figure 8a) interconversion between the two conformers ceases by 0.8 GPa. The population of minor conformers at this pressure, however, is not reduced to zero as can be seen from Figure 8b. There exists a significant population of minor conformers (around 12%) at site 1. As already noted our previous study[9] has shown that the activation energy for pedal motion is 14.68 kJ/mol at site 1 at atmospheric pressure. At higher pressures, the activation energy is expected to be still higher. This leads to reduction in interconversion rate to zero even before the population of minor conformers has been reduced to zero. This situation may not arise if the pressure is increased gradually which is time-consuming in a simulation but can be easily achieved in an experiment. Thus, slower increase in pressure can probably lead to zero population of minor conformers at site 1. From our previous study,[9] we know $E_{a2} = 10.38$ kJ/mol and $E_{a1} > E_{a2}$. Increase in pressure is likely to lead to increase in activation energy due to decrease in intermolecular distances. This is evident from a plot of $U_{\text{total}}(\phi)$ for various pressures (see Figure 9). Note that the difference in U_{total} between major conformer ($\phi = 0°$) and transition states ($\phi = \pm 90°$) increases with pressure. By 1.25 GPa this difference is more than a few times k_BT, the kinetic energy at room temperature. Thus, at higher pressures pedallike motion is completely absent. The lower activation energy of the molecules at site 2 enables all the minor conformers to change over to major conformers. Larger activation energy at site 1 prohibits all the minor conformers to change to major conformers. Figure 9 shows major conformers have more favorable interaction energies than minor conformers. Figure 10 shows a snapshot of stilbene crystal at two different pressures (1 atm and 4.0 GPa) at 300K. At 1 atm as is evident from Figure 10a there is a large degree of *dynamic disorder*.

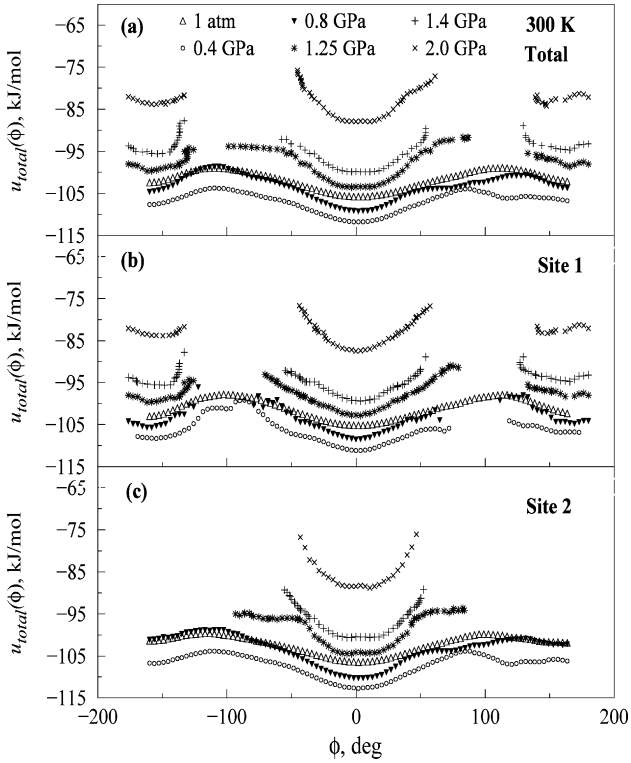

Figure 9. $u(\phi)$ as a function of pressure averaged over (a) both the crystallographic sites, (b) site 1, (c) site 2.

This coexists with considerable degree of *static disorder* which is essentially the minor conformer. At 4.0 GPa, the crystal exhibits a considerable degree of order. However, we can see some degree of disorder in the crystal. This is mainly static disorder with little or no dynamic disorder. From the $U_{\text{total}}(\phi)$ (see Figure 9), it is clear that minor conformers exist at a local potential minimum leading to a long lifetime. By 1.4 GPa, the static disorder disappears completely at site 2 which is not the case at site 1. However, the dynamic disorder disappears completely both at site 1 and site 2 by 1.5 GPa itself. We have attempted to look at possible thermodynamic signature of the freezing of conformational interconversion in stilbene as a function of pressure. As already discussed a slight lowering in the derivative, $d(V/V_0)/dP$ is seen around 1.25 GPa. In Figure 11, we show a plot of specific heat at constant pressure, C_P as a function of pressure. C_P has been calculated from the usual expression.

$$C_P = \frac{\langle H^2 \rangle - \langle H \rangle^2}{k_B T^2} \tag{4}$$

Here, H is enthalpy and given by $H = U_{\text{total}} + PV$ where P is the pressure and V the volume. A maximum is seen at around the same pressure (1.25 GPa) in C_P also. It is likely that maximum in C_P and $d(V/V_0)/dP$ are associated with disappearance of interconversion between minor and major conformers at site 2. The nature of this transition appears to be higher than first order.

The pressure at which the transition takes place is crucially dependent on the intermolecular potential. Our temperature dependent study indicates that simulation results are somewhat different from those of the experiments indicating that the potential employed here is approximate. Thus, the transition pressure obtained here may not be what one will find experimentally. Further, a characteristic change in thermodynamic

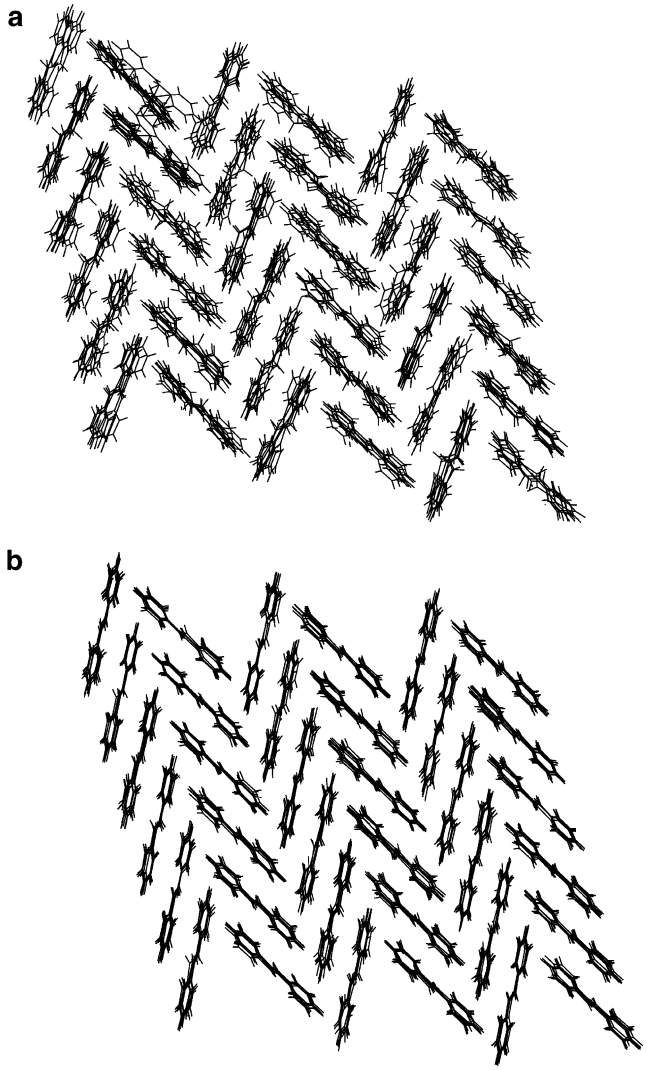

Figure 10. Snapshot along *b* axis at (a) 1 atm, 300 K, (b) 4.0 GPa, 300 K.

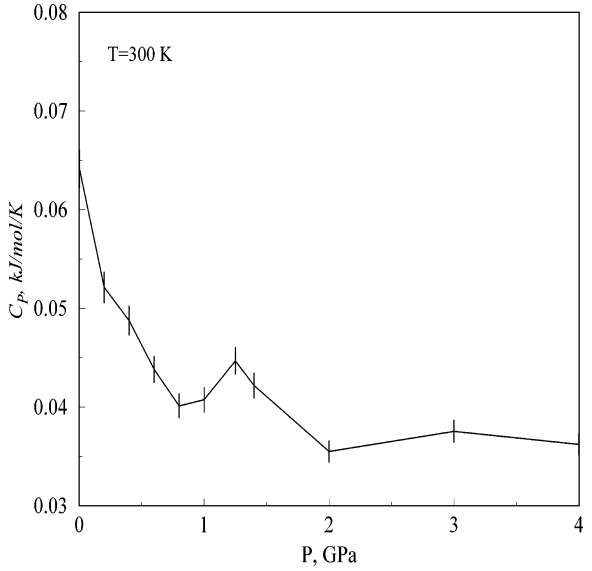

Figure 11. Variation of C_P as a function of pressure with error bars.

properties due to complete absence of interconversion at site 1 should also be seen in an experiment, although this may be less pronounced than seen for site 2, since the population of minor conformer is lower at site 1. Our calculations have not shown any such signature associated with motion at site 1 possibly because of this reason.

In our calculations, due to rapid increase in pressure we have found that minor conformer of stilbene at site 1 does not transform into the major conformer. But if the pressure is increased sufficiently slowly which can be easily achieved experimentally, then it is likely that a signature of this would be seen in C_P. Thus, it appears that the two transitions seen by us, although not exactly at the same pressure as the pressure reported by Takeshita et al,[12] are still related to each other. Our calculations suggest that the two transitions seen in Raman studies probably have their origin in the disappearance of disorder (minor conformer) at sites 1 and 2 and absence of pedallike motion at these sites. The pressures at which we see the transitions in our calculations are likely to be not accurate because the intermolecular potential employed by us here do not predict the other known experimental quantities such as lattice parameters correctly and also because of the rapid increase in pressure in the calculations. In summary, we find that the results of the present study suggest existence of two transitions, possibly second order, in agreement with the findings based on Raman measurements by Takeshita et al.[12] although due to certain limitation inherent to the computational technique we have not been able to see both the transitions. Further, our present study provides additional microscopic insight into the nature or origin of these transitions: the two transitions have their origin in the disappearance of the pedallike motion at the two crystallographic sites. We note that the rate of change in pressure or temperature in the simulation is typically several orders of magnitude higher than typical employed in experiment and that these can lead to transition pressure/temperatures which are higher than experiment.[30,31]

5. Conclusions

Increase in hydrostatic pressure on stilbene crystals at 300 K leads to a significant decrease in lattice parameters and volume of the unit cell. We have shown that this large (25%) decrease in unit cell volume is due to an increase in the planarity of the molecules. Further the pedallike motion decreases as a consequence of increased activation energy for $\phi = \pm 90°$ conformations. While the population of minor conformers at site 2 vanishes those at site 1 shows hardly any decrease. This is surprising and is probably due to larger activation energy for pedallike motion for molecules at site 1. Both compressibility and specific heat show signature of a transition around 1.25 GPa. This seems to be associated with the complete disappearance of minor conformers at site 2. Thus, at high pressures (>2.0 GPa), there is complete disappearance of dynamic disorder arising from pedallike motion, but their remains some degree of static disorder. The static disorder arises from the presence of 12% minor conformers at site 1. The transitions reported by Takeshita et al.[12] based on Raman measurements at 1.5−2 and 4 GPa probably have arisen from disappearance of minor conformers at the two crystallographic sites.

Acknowledgment. The authors wish to gratefully acknowledge the Department of Science and Technology, New Delhi, and BRNS, Mumbai, for financial support. Financial support from JNCASR is also gratefully acknowledged. Authors wish to thank Dr. P. C. Jha for useful discussions.

References and Notes

(1) Price, D. L.; Saboungi, M.-L.; Bermejo, F. J. *Rep. Prog. Phys.* **2003**, *66*, 407.

(2) Mott, N. F. *Philos. Mag.* **1966**, *13*, 93.
(3) Anderson, P. W.; Halperin, B. C.; Varma, C. M. *Philos. Mag.* **1972**, *25*, 1.
(4) Abrahams, S. C. *Acta Crystallogr., Sect. A* **1994**, *50*, 658.
(5) Bernstein, J.; Mirsky, K. *Acta Crystallogr., Sect. A* **1978**, *34*, 161.
(6) Harada, J.; Ogawa, K. *J. Am. Chem. Soc.* **2001**, *123*, 10884.
(7) Ogawa, K.; Sano, T.; Yoshimura, S.; Takeuchi, Y.; Toriumi, K. *J. Am. Chem. Soc.* **1992**, *114*, 1041.
(8) Galli, S.; Mercandelli, P.; Sironi, A. *J. Am. Chem. Soc.* **1999**, *121*, 3767.
(9) Murugan, N. A.; Yashonath, S. *J. Phys. Chem. B.* **2004**, *108*, 17403.
(10) Ghoshal, S. K.; Sarkar, S. K.; Kastha, G. S. *Mol. Cryst. Liq. Cryst.* **1983**, *91*, 1.
(11) Chakrabarti, S.; Misra, T. N. *Bull. Chem. Soc. Jpn.* **1991**, *64*, 2454.
(12) Takeshita, H.; Suzuki, Y.; Hirai, y.; Nibu, Y.; Shimada, H.; Shimada, R. *Bull. Chem. Soc. Jpn.* **2004**, *77*, 477.
(13) Parrinello, M.; Rahman, A. *Phys. Rev. Lett.* **1980**, *45*, 1196.
(14) Nose, S.; Klein, M. L. *J. Chem. Phys.* **1983**, *78*, 6928.
(15) Bounds, D. G.; Klein, M. L.; Patey, G. N. *J. Chem. Phys.* **1980**, *72*, 5348.
(16) Nose, S.; Klein, M. L. *Phys. Rev. Lett.* **1983**, *50*, 1207.
(17) Klein, M. L.; McDonald, I. R. *Chem. Phys. Lett.* **1981**, *80*, 76.
(18) Tse, J. S.; Klein, M. L. *Phys. Rev. Lett.* **1987**, *58*, 1672.
(19) Allen, M. P.; Tildesley, D. J. *Computer Simulation of Liquids*; Clarendon Press: Oxford, 1987.
(20) Frenkel, D.; Smit, B. *Understanding Molecular Simulations*; Academic Press: San Diego, 1996.
(21) Velardez, G. F.; Alavi, S.; Thompson, D. L. *J. Chem. Phys.* **2003**, *119*, 6698.
(22) Sprik, M.; Rothlisberger, U.; Klein, M. L. *J. Phys. Chem. B.* **1997**, *101*, 2745.
(23) Grieg, D. W.; Pawley, G. S. *Mol. Phys.* **1996**, *89*, 677.
(24) Williams, D. E. *J. Mol. Str.* **1999**, *485*−*486*, 321.
(25) Yashonath, S.; Price, S. L.; McDonald, I. R. *Mol. Phys.* **1988**, *64*, 361.
(26) Frisch, M. J.; et al., *Gaussian 98*, Revision A.9; Gaussian, Inc.: Pittsburgh, PA, 1998.
(27) Metropolis, N.; Rosenbluth, A. W.; Rosenbluth, M. N.; Teller, A. H.; Teller, E. *J. Chem. Phys.* **1953**, *21*, 1087.
(28) Yashonath, S.; Rao, C. N. R. *Chem. Phys. Lett.* **1985**, *119*, 22.
(29) Hoekstra, A.; Meertens, P.; Vos, A. *Acta Crystallogr. Sect. B.* **1975**, *31*, 2813.
(30) Murugan, N. A.; Jha, P. C.; Yashonath, S.; Ramasesha, S. *J. Phys. Chem. B.* **2004**, *108*, 4178.
(31) Murugan, N. A.; Yashonath, S. *J. Phys. Chem. B.* **2005**, *109*, 2014.
(32) Murugan, N. A.; Yashonath, S. *J. Phys. Chem. B.* **2005**, *109*, 1433.
(33) Harada, J.; Ogawa, K. *J. Am. Chem. Soc.* **2001**, *123*, 10884.
(34) Harada, J.; Ogawa, K. *J. Am. Chem. Soc.* **2004**, *126*, 3539.
(35) Luo, S.-N.; Ahrens, T. J. *Appl. Phys. Lett.* **2003**, *82*, 1836.
(36) Lu, K.; Li, Y. *Phys. Rev. Lett.* **1998**, *80*, 4474.